ISSN 1063-7710, Acoustical Physics, 2023, Vol. 69, No. 4, pp. 436–441. © Pleiades Publishing, Ltd., 2023.

CLASSICAL PROBLEMS OF LINEAR ACOUSTICS AND WAVE THEORY

Mode-Matching Analysis for Sound Propagation in a Cylindrical Duct with a Partial Lining

B. Tiryakioglu[a], * and H. Ozturk[b]

[a] *Department of Applied Mathematics, Marmara University, Istanbul, 34722 Turkey*

[b] *Department of Mathematics, Gebze Technical University, Kocaeli, 41400 Turkey*

**e-mail: burhan.tiryakioglu@marmara.edu.tr*

Received November 18, 2020; revised February 17, 2023; accepted March 16, 2023

Abstract—A mode-matching analysis of infinite cylindrical duct with a partial absorbing internal surface is considered. The solution for the field terms are determined in form of eigenmodes which are matched across the boundary of each junction discontinuity. Numerical results are performed to show the influence of the different parameters such as waveguide radius, length of the lined part and acoustic absorbing lining on the propagation phenomenon. The method is also compared with the Wiener–Hopf technique which is more difficult to implement and very good corroboration is observed.

Keywords: mode-matching technique, absorbent lining, circular duct, acoustics, wave propagation

DOI: 10.1134/S1063771023600274

1. INTRODUCTION

Motors, jet fans and blowers produce a great deal of noise on a daily basis. Unfortunately, increasing noise pollution impacts millions of people and presents a serious risk to their health. For this reason, the propagation of acoustic waves has received increasing attention due to its importance in reduction of noise pollution.

The widely accepted method for reducing sound by researchers is the use of silencers. Silencers can be classified into two types as reactive and dissipative. Reactive silencers are designed to reflect sound back to the source by means of sudden changes on the geometry while dissipative silencers use acoustically absorbing materials to attenuate sound waves. To reveal the effect of these silencers, lots of publications have been developed extensively in the past. Several analytical techniques such as Fourier method, Wiener–Hopf technique and mode-matching technique have been studied by many investigators [1–7]. Morse [8], Cremer [9] and Lapin [10] included an infinite closed duct as their models and studied the effects of the acoustically absorbent lining on sound transmission. Then, Rawlins [11] provided a Wiener-Hopf solution to the problem where the interior surface of the semi-infinite tube is assumed to be acoustically lined. Transfer matrix formulation, which has been utilized in low frequency analysis, was also derived by Peat [12] for the extended inlet or outlet duct systems as a reactive silencer. In addition, Tiryakioglu et al., [13] used mode-matching approach in conjunction with the Wiener–Hopf technique to model a dissipative silencer and examined the partially lined duct.

In mode matching technique, which is based on dividing geometry into different regions, the unknown fields are expressed in terms of eigenmodes which are satisfying the appropriate boundary conditions in each region. These unknown fields are obviously determined by considering the continuity conditions at the junctions. Then, these fields containing an infinite number of unknown coefficients are solved numerically. The mode matching technique which has been applied in many scattering problems, is easy to implement and give accurate results. Hassan et al., [14] considered the mode matching analysis for wave scattering in triple and pentafurcated spaced ducts. Hassan and Bashir then treated a similar problem with soft outer lining [15]. They studied five spaced waveguide problem. Recently, the mode matching analysis for two-dimensional acoustic wave propagation in a trifurcated lined duct was investigated by Khalid et al., [16].

In the present work the effect of partial absorbing internal surface on propagation of sound waves along cylindrical duct is investigated. The mode-matching method is applied to the problem and infinite system of linear algebraic equations obtained by considering boundary conditions and continuity relations. Then, this system is solved for the prediction of reflection and transmission coefficients. Some numerical results showing the influence of the internal surface impedance and length of the impedance loading are pre-

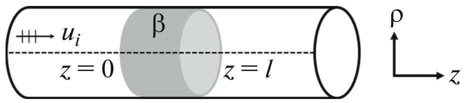

Fig. 1. Geometry of the problem.

sented. Also, the results from the current study are compared with the study of [17] and [18] which are solved with the Wiener–Hopf technique. For different values of the absorbing lining, excellent corroboration is observed. The results we have presented in this paper demonstrate the significance of the finite coating and would be beneficial in constructing dissipative silencers.

2. FORMULATION OF THE WAVEGUIDE PROBLEM

Consider the incident field propagating along a waveguide with a partial absorbing lining, as shown in Fig. 1, given by

$$u_i(z) = e^{ikz}. \tag{1}$$

Duct walls are assumed to be infinitely thin and they occupy the region $\{\rho = a, z \in (-\infty, \infty)\}$. The partial $(0 < z < l)$ inner surface of cylinder is assumed to be lined with acoustically absorbing material. The liner impedance is denoted by Z. In Fig. 1, $\beta = \rho_0 c/Z$ is the specific admittance where c is the velocity of sound. From the symmetry of the geometry of the problem and of the incident wave, the total field is taken independent of ϕ everywhere in circular cylindrical coordinate system (ρ, ϕ, z). We shall therefore introduce a scalar potential $u(\rho, z)$ which defines the acoustic pressure and velocity by $p = i\omega\rho_0 u$ and $v = \operatorname{grad} u$, respectively, where ρ_0 is the density of undisturbed medium. The time dependence is assumed to be $e^{-i\omega t}$ and suppressed through the paper, where ω is the angular frequency.

In order to simplify the solution, it is possible to define the total field $u^T(\rho, z)$ as a piecewise function as shown below

$$u^T(\rho, z) = \begin{cases} u_1(\rho, z) + u_i(z), & \rho < a, z \in (-\infty, 0), \\ u_2(\rho, z) & , \quad \rho < a, z \in (0, l), \\ u_3(\rho, z) & , \quad \rho < a, z \in (l, \infty), \end{cases} \tag{2}$$

where $u_1(\rho, z)$, $u_2(\rho, z)$ and $u_3(\rho, z)$ denote the unknown fields in their relevant regions. The field terms satisfy the below boundary conditions.

$$\frac{\partial}{\partial\rho} u_1(a, z) = 0, \quad -\infty < z < 0, \tag{3}$$

$$\left(ik\beta - \frac{\partial}{\partial\rho}\right) u_2(a, z) = 0, \quad 0 < z < l, \tag{4}$$

$$\frac{\partial}{\partial\rho} u_3(a, z) = 0, \quad l < z < \infty. \tag{5}$$

Also, in addition to the boundary conditions given by (3)–(5), the following edge conditions apply to ensure the uniqueness of the problem under consideration [19]:

$$u^T(\rho, z) = O(1), \quad z \to 0, \tag{6}$$

$$\frac{\partial}{\partial\rho} u^T(\rho, z) = O(z^{-1/2}), \quad z \to 0, \tag{7}$$

$$u^T(\rho, z) = O(1), \quad z \to l, \tag{8}$$

$$\frac{\partial}{\partial\rho} u^T(\rho, z) = O\left((z-l)^{-1/2}\right), \quad z \to l. \tag{9}$$

3. SOLUTION OF THE WAVEGUIDE PROBLEM

We divide our waveguide into three regions for solving the problem with the mode-matching technique. First, we determine the eigenfunction expansions in cylindrical waveguides and related orthogonality conditions in each waveguide region [20].

3.1. Region I $\{-\infty < z < 0\}$

Let's solve the given problem in various regions by applying the eigenfunctions expansion. The solution in this region can be written as

$$u_1(\rho, z) = \sum_{n=1}^{\infty} R_n e^{-i\alpha_n z} J_0(j_n \rho/a), \tag{10}$$

where R_n is the amplitude of the reflected duct mode in region I. Here where J_n is the Bessel function of order n, j_n is the root of the equation

$$J_1(j_n) = 0, \quad n = 1, 2, \ldots \tag{11}$$

and α_n stands for

$$\alpha_n = \sqrt{k^2 - (j_n/a)^2}, \tag{12}$$

By using the following Lommel integral formulas [21], we get

$$\int_0^a [J_0(j_n \rho/a)]^2 \rho d\rho = \frac{a^2}{2} J_0^2(j_n). \tag{13}$$

3.2. Region II $\{0 < z < l\}$

In this region $u_2(\rho, z)$ can be expressed as

$$u_2(\rho, z) = \sum_{n=1}^{\infty} [A_n e^{i\chi_n z} + B_n e^{-i\chi_n z}] J_0(\tau_n \rho/a), \tag{14}$$

where τ_n is the root of the equation

$$ika\beta J_0(\tau_n) + \tau_n J_1(\tau_n) = 0, \quad n = 1,2,... \tag{15}$$

and χ_n stands for

$$\chi_n = \sqrt{k^2 - (\tau_n/a)^2}. \tag{16}$$

The $J_0(\tau_n\rho/a)$ satisfy the relation [22]

$$\int_0^a \left[J_0\left(\tau_n\rho/a\right)\right]^2 \rho d\rho = \frac{a^2}{2}[J_0^2(\tau_n) + J_1^2(\tau_n)] = P_n. \tag{17}$$

3.3. Region III $\{l < z < \infty\}$

For this region, the transmitted field can be written as

$$u_3(\rho, z) = \sum_{n=1}^{\infty} T_n e^{i\alpha_n z} J_0(j_n\rho/a), \tag{18}$$

where T_n is the amplitude in region III. Here j_n and α_n are given in (11) and (12) respectively.

4. FORMULATION OF THE INFINITE SET OF EQUATIONS

We apply the mode-matching technique by using continuity relations at $z = 0$ and $z = l$. First, the following equations are obtained at $z = 0$

$$\frac{\partial}{\partial z}u_2(\rho,0) = \frac{\partial}{\partial z}u_1(\rho,0) + \frac{\partial}{\partial z}u_i(0), \tag{19}$$

$$u_2(\rho,0) = u_1(\rho,0) + u_i(0). \tag{20}$$

Substituting (10) and its derivative with respect to z into (14), we obtain

$$i\sum_{n=1}^{\infty}\chi_n[A_n - B_n]J_0(\tau_n\rho/a) = -i\sum_{m=1}^{\infty}R_m\alpha_m J_0(j_m\rho/a) + ik, \tag{21}$$

$$\sum_{n=1}^{\infty}[A_n + B_n]J_0(\tau_n\rho/a) = \sum_{m=1}^{\infty}R_m J_0(j_m\rho/a) + 1. \tag{22}$$

By following a similar procedure described in [22, 23], we can take an integral over $[0, a]$ after multiplying the both sides of equation (19) and (20) with $\rho J_0(\tau_n\rho/a)$ and using (17), we get

$$[A_n - B_n]\chi_n P_n = -a^2\tau_n J_1(\tau_n)\sum_{m=1}^{\infty}R_m\alpha_m\frac{J_0(j_m)}{\tau_n^2 - j_m^2} + a^2k\frac{J_1(\tau_n)}{\tau_n}, \tag{23}$$

$$[A_n + B_n]P_n = a^2\tau_n J_1(\tau_n)\sum_{m=1}^{\infty}R_m\frac{J_0(j_m)}{\tau_n^2 - j_m^2} + a^2\frac{J_1(\tau_n)}{\tau_n}. \tag{24}$$

A_n and B_n can be obtained from (23) and (24) as

$$A_n = \frac{a^2\tau_n J_1(\tau_n)}{2\chi_n P_n}\left[\sum_{m=1}^{\infty}R_m\frac{\chi_n - \alpha_m}{\tau_n^2 - j_m^2}J_0(j_m) + \frac{\chi_n + k}{\tau_n^2}\right], \tag{25}$$

$$B_n = \frac{a^2\tau_n J_1(\tau_n)}{2\chi_n P_n}\left[\sum_{m=1}^{\infty}R_m\frac{\chi_n + \alpha_m}{\tau_n^2 - j_m^2}J_0(j_m) + \frac{\chi_n - k}{\tau_n^2}\right]. \tag{26}$$

Similarly, from the continuity relations at $z = l$, we obtain

$$\frac{\partial}{\partial z}u_2(\rho,l) = \frac{\partial}{\partial z}u_3(\rho,l), \tag{27}$$

$$u_2(\rho,l) = u_3(\rho,l). \tag{28}$$

By using (14) together with (18), we get the following equations

$$\sum_{n=1}^{\infty}\chi_n[A_n e^{i\chi_n l} - B_n e^{-i\chi_n l}]J_0(\tau_n\rho/a) = \sum_{m=1}^{\infty}T_m\alpha_m e^{i\alpha_m l}J_0(j_m\rho/a), \tag{29}$$

$$\sum_{n=1}^{\infty}[A_n e^{i\chi_n l} + B_n e^{-i\chi_n l}]J_0(\tau_n\rho/a) = \sum_{m=1}^{\infty}T_m e^{i\alpha_m l}J_0(j_m\rho/a). \tag{30}$$

A_n and B_n can be obtained easily as follows

$$A_n = \frac{a^2\tau_n J_1(\tau_n)}{2\chi_n P_n}\sum_{m=1}^{\infty}T_m\frac{\chi_n + \alpha_m}{\tau_n^2 - j_m^2}J_0(j_m)e^{i(\alpha_m - \chi_n)l}, \tag{31}$$

$$B_n = \frac{a^2\tau_n J_1(\tau_n)}{2\chi_n P_n}\sum_{m=1}^{\infty}T_m\frac{\chi_n - \alpha_m}{\tau_n^2 - j_m^2}J_0(j_m)e^{i(\alpha_m + \chi_n)l}. \tag{32}$$

We can simplify these equations as follows. From (25)–(26) and (31)–(32), we have

$$\sum_{m=1}^{\infty}T_m\frac{\chi_n + \alpha_m}{\tau_n^2 - j_m^2}J_0(j_m)e^{i(\alpha_m - \chi_n)l} - \sum_{m=1}^{\infty}R_m\frac{\chi_n - \alpha_m}{\tau_n^2 - j_m^2}J_0(j_m) = \frac{\chi_n + k}{\tau_n^2}, \tag{33}$$

$$\sum_{m=1}^{\infty}T_m\frac{\chi_n - \alpha_m}{\tau_n^2 - j_m^2}J_0(j_m)e^{i(\alpha_m + \chi_n)l} - \sum_{m=1}^{\infty}R_m\frac{\chi_n + \alpha_m}{\tau_n^2 - j_m^2}J_0(j_m) = \frac{\chi_n - k}{\tau_n^2}. \tag{34}$$

R_m and T_m can be determined by solving the linear systems (33) and (34) numerically.

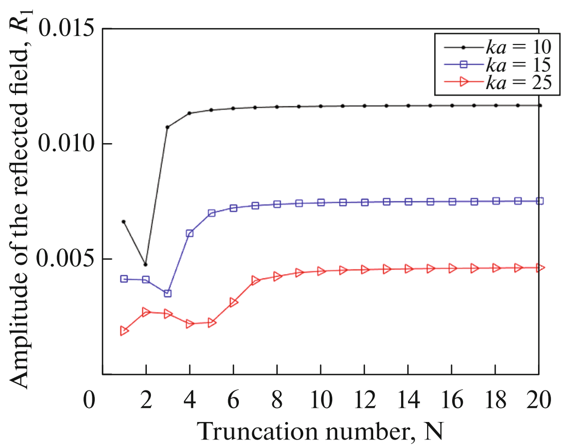

Fig. 2. Amplitude of the reflected field versus the truncation number N with $kl = 10$ and $\beta^{-1} = 1 - 3i$.

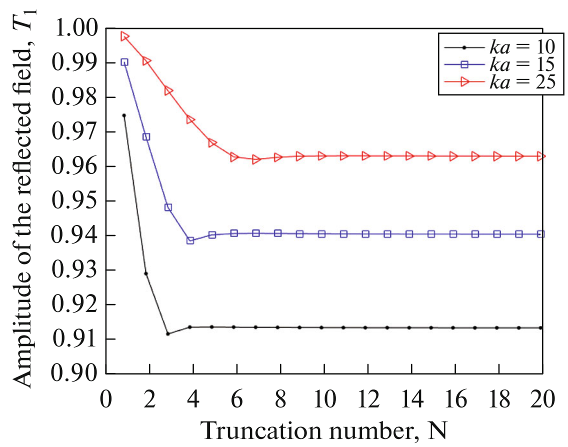

Fig. 3. Amplitude of the transmitted field versus the truncation number N with $kl = 10$ and $\beta^{-1} = 1 - 3i$.

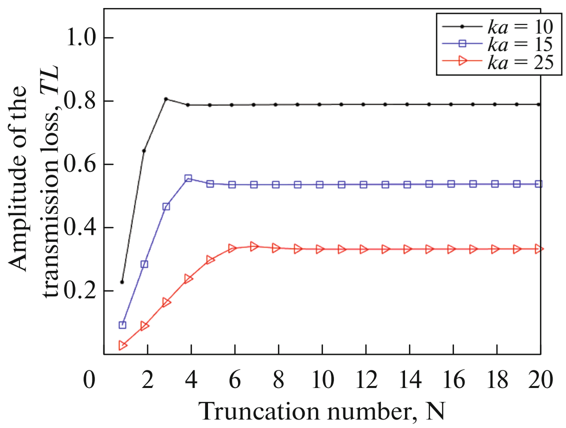

Fig. 4. Amplitude of the transmission loss versus the truncation number N with $kl = 10$ and $\beta^{-1} = 1 - 3i$.

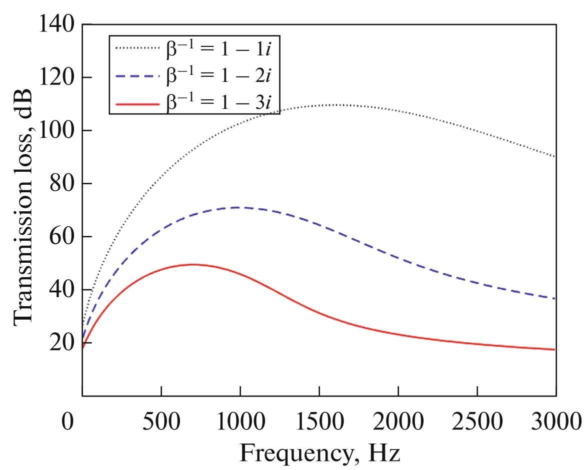

Fig. 5. Transmission loss versus impedance with $a = 0.025$ m, $l = 0.5$ m.

5. NUMERICAL RESULTS

In order to show the effects of the parameters like the duct radius a, the length l of the lining and the surface impedance β^{-1} on the radiation phenomenon, some numerical results showing variation of the reflection coefficient R_1, the transmission coefficient T_1 and the transmission loss TL with different parameters are presented. Transmission loss is obtained by using the following formula [18]

$$TL = -20\log_{10}|T_1|.$$

The values of dimensionless ka and kl are taken from the study of [17, 18] while the absorbing lining is taken from [1, 24]. The numerical results are carried out for the dominant mode in the waveguide and by truncating the infinite series and the infinite systems of linear algebraic equations after the first N terms. Figures 2–4 show the amplitude of the reflected, transmitted fields and transmission loss for $kl = 10$ and $\beta^{-1} = 1 - 3i$. It is seen that the infinite series converge rapidly enough to truncate it after the first few terms. The truncation number is chosen as $N = 10$.

Figures 5 and 6 illustrate the effect of the surface impedance on the transmission loss. It is seen that transmission loss can be reduced by changing the values of real and imaginary part of the surface impedance.

Figures 7 and 8 show the dependence of the transmission loss to the radius a and lining length l. When a increases, the transmission loss decreases. On the

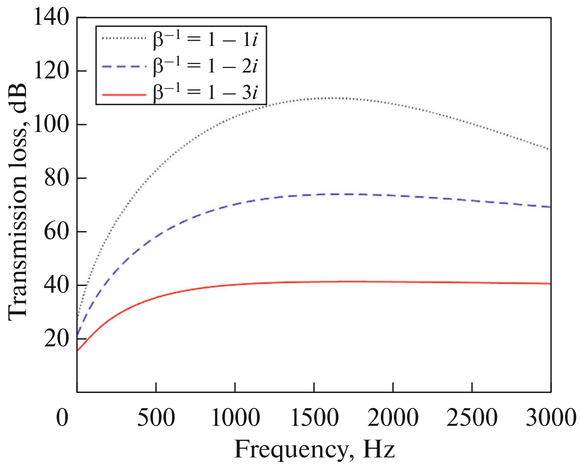

Fig. 6. Transmission loss versus impedance with $a = 0.025$ m, $l = 0.5$ m.

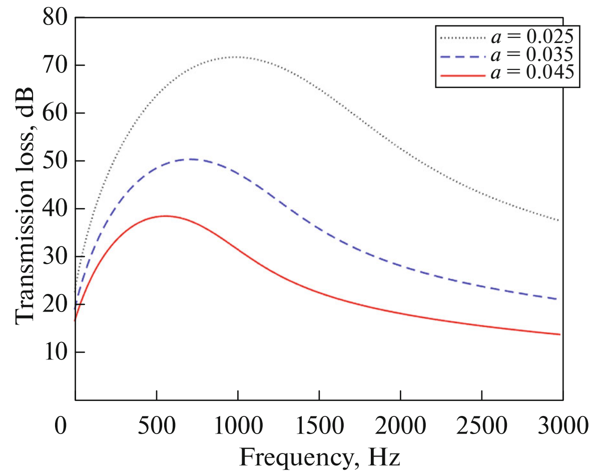

Fig. 7. Transmission loss versus duct radius with $l = 0.5$ m, $\beta^{-1} = 1 - 2i$.

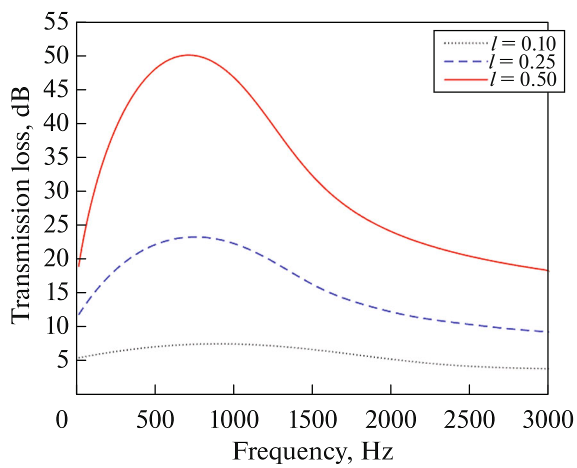

Fig. 8. Transmission loss versus lining length with $a = 0.025$ m, $\beta^{-1} = 1 - 3i$.

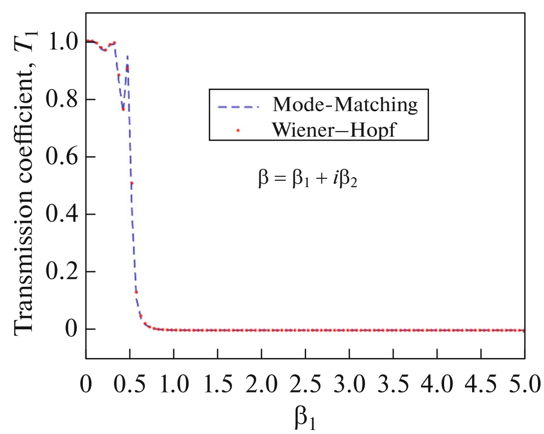

Fig. 9. Comparison of the transmission coefficient with $ka = 1$ and $kl = 10$.

contrary, incremental transmission loss occurs for an increasing values of l.

Finally, the numerical results are corroborated with the studies [17] and [18] where the problems are solved by using Wiener–Hopf method, respectively. Figure 9 represents the graph of transmission coefficient against the real part of the impedance for the Wiener–Hopf technique and mode-matching technique. Figure 10 denotes the transmission loss for $\beta = 0.5i$ and $\beta = 0.9i$, calculated using the techniques mode-matching and Wiener–Hopf with zero Mach number. For the comparison, we assumed that the expansion chamber radius goes to duct radius in [17] and [18]. Results exhibit two approaches have a good agreement.

6. CONCLUSIONS

Cylindrical duct with a finite lining on the wall have been studied rigorously. The problem is solved by using the mode-matching technique. In the solution, infinite number of unknown coefficients, which satisfy an infinite set of linear algebraic equations, are involved and solved numerically. On the other hand, the results have been compared with the Wiener–Hopf technique. It is shown that very good agreement is obtained. This knowledge is very important, because in more complicated problems, where the

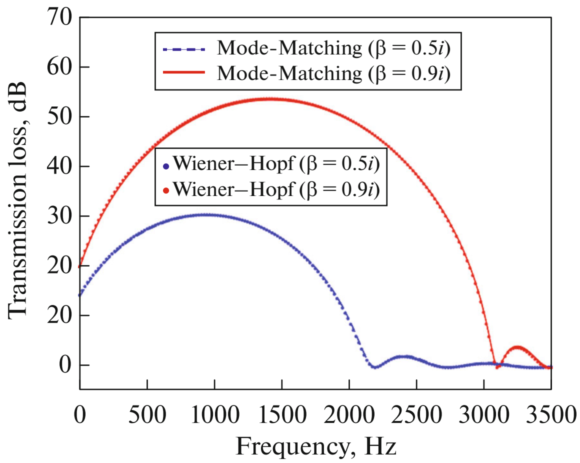

Fig. 10. Comparison of the transmission loss with $a = 0.0243$ and $l = 0.21981$.

Wiener–Hopf technique cannot be practicable, the mode-matching method can be used. In particular, it is observed that there is a remarkable reduction in the transmission which is possible for certain parameters. These results can be useful in acoustic analysis for dissipative silencers.

CONFLICT OF INTEREST

The authors declare that they have no conflicts of interest.

REFERENCES

1. B. Tiryakioglu, Acta Acust. Acust. **105** (4), 591 (2019). https://doi.org/10.3813/AAA.919340
2. B. Tiryakioglu, J. Eng. Math. **122** (1), 17 (2020). https://doi.org/10.1007/s10665-020-10042-x
3. L. Huang, J. Acoust. Soc. Am. **112** (5), 2014 (2002). https://doi.org/10.1121/1.1508778
4. H. Ozturk, TWMS J. Appl. Eng. Math. **10** (3), 690 (2020)
5. G. Cinar, H. Ozturk, and O. Y. Cinar, Math. Method Appl. Sci. **34** (2), 220 (2011). https://doi.org/10.1002/mma.1351
6. R. F. Huang and D. M. Zhang, Pier **67**, 205 (2007). https://doi.org/10.2528/PIER06083103
7. S. Shafique, M. Afzal, and R. Nawaz, Can. J. Phys. **95** (6), 581 (2017). https://doi.org/10.1139/cjp-2016-0801
8. P. M. Morse, J. Acoust. Soc. Am. **11** (2), 205 (1939). https://doi.org/10.1121/1.1916024
9. L. Cremer, Acustica **3**, 249 (1953).
10. A. D. Lapin, Sov. Phys. Acoust. **21** (3), 215 (1975).
11. A. D. Rawlins, Proc. R. Soc. London A **361**, 65 (1978). https://doi.org/10.1098/rspa.1978.0092
12. K. S. Peat, J. Sound Vib. A **150** (1), 101 (1978). https://doi.org/10.1016/0022-460X(91)90404-8
13. B. Tiryakioglu and A. Demir, Arch. Acoust. **44** (2), 239 (2019). https://doi.org/10.24425/aoa.2019.128487
14. M. Hassan, M. H. Meylan, A. Bashir, and M. Sumbul, Math. Method Appl. Sci. **39** (11), 3043 (2016). https://doi.org/10.1002/mma.3751
15. M. Hassan and A. Bashir, Can. J. Phys. **96** (2), 165 (2017). https://doi.org/10.1139/cjp-2017-0045
16. A. Khalid, S. Younas, I. Khan, R. Manzoor, R. Nawaz, and E. M. Sherif, J. Interdiscip. Math. **22** (7), 1095 (2020). https://doi.org/10.1080/09720502.2019.1706888
17. A. Demir and A. Buyukaksoy, Int. J. Eng. Sci. **41** (20), 2411 (2003). https://doi.org/10.1016/S0020-7225(03)00240-4
18. A. Demir and A. Buyukaksoy, Int. J. Eng. Sci. **45** (3), 398 (2005). https://doi.org/10.1016/j.ijengsci.2004.12.003
19. R. Mittra and S. W. Lee, *Analytical Techniques in the Theory of Guided Waves* (Macmillan Co., 1971).
20. C. Y. Lo and R. V. Churchill, *Boundary Value Problems* (World Sci., 2000), Chapter 7.
21. A. Isikyer and A. Demir, Bull. Tech. Univ. Istanbul **54** (5), 46 (2007).
22. A. Demir and A. Buyukaksoy, Acta Acust. Acust. **89** (4), 578 (2003).
23. J. W. Brown and R. V. Churchill, *Fourier Series and Boundary Value Problems,* 5th ed. (McGraw-Hill, Inc., 1993), Chapter 7.
24. N. Peake and I. D. Abrahams, Wave Motion **92**, 102407 (2020). https://doi.org/10.1016/j.wavemoti.2019.102407